UCRL-ID-128841

Electrical Resistivity Monitoring of the Single Heater Test in Yucca Mountain

A. Ramirez
W. Daily

October 1997

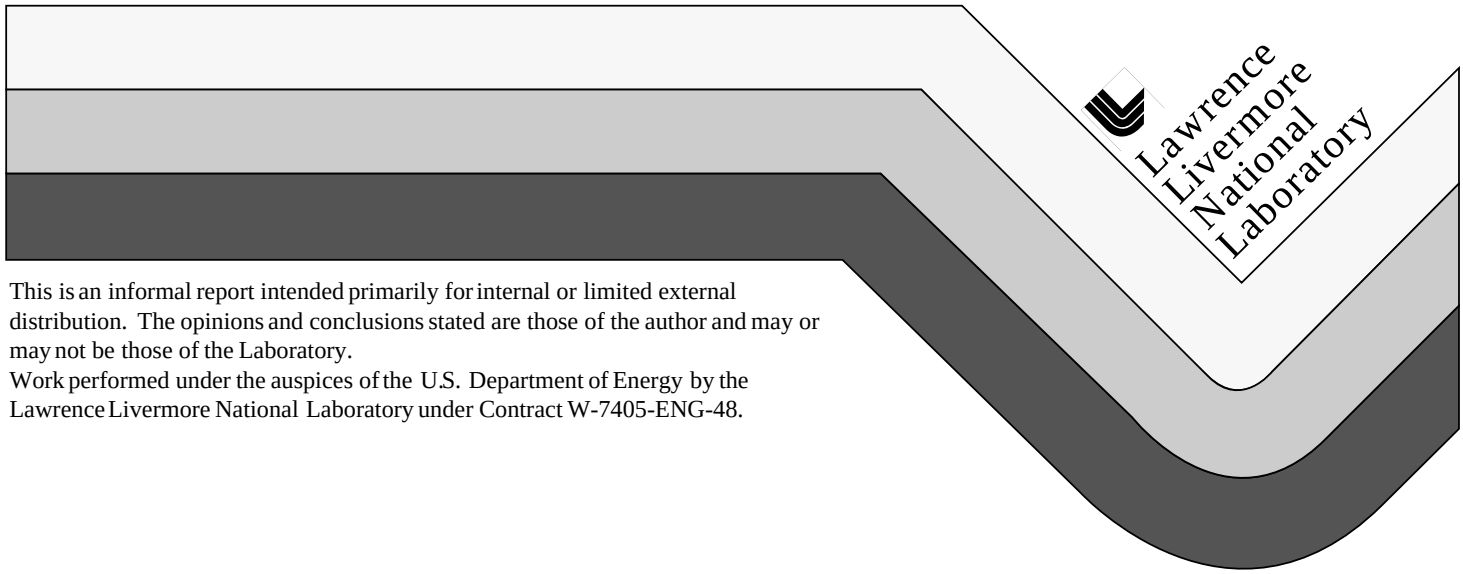

Work performed under the auspices of the U.S. Department of Energy by the Lawrence Livermore National Laboratory under Contract W-7405-ENG-48.

Electrical Resistivity Monitoring of the Single Heater Test in Yucca Mountain

A. Ramirez, W. Daily
Lawrence Livermore National Laboratory

Abstract: Of the several thermal, mechanical and hydrological measurements being used to monitor the rockmass response in the Single Heater Test, electrical resistance tomography (ERT) is being used to monitor the movement of liquid water with a special interest in the movement of condensate out of the system. Images of resistivity change were calculated using data collected before, during and after the heating episode. This report will concentrate on the results obtained after heating ceased; previous reports discuss the results obtained during the heating phase. The changes recovered show a region of increasing resistivity approximately centered around the heater as the rock mass cooled. The size of this region grows with time and the resistivity increases become stronger. The increases in resistivity are caused by both temperature and saturation changes. The Waxman Smits model has been used to calculate rock saturation after accounting for temperature effects. The saturation estimates suggest that during the heating phase, a region of drying forms around the heater. During the cooling phase, the dry region has remained relatively stable. Wetter rock regions which developed below the heater during the heating phase, are slowly becoming smaller in size during the cooling phase. The last set of images indicate that some rewetting of the dry zone may be occurring. The accuracy of the saturation estimates depends on several factors that are only partly understood.

Introduction

The Single Heater Test (SHT) is one of the in situ thermal tests being conducted in the exploratory studies facility (ESF) in Yucca Mountain to enhance the understanding of the coupled processes. The primary objective of the SHT is to investigate the thermal-mechanical responses of the Topopah Spring tuff in Yucca Mountain.

This paper describes electrical resistance tomography (ERT) surveys made during the SHT in order to map the changes in moisture content caused by heating. Of particular interest, is the formation and movement of condensate within the fractured rock mass. In this report, we concentrate on the results observed during the fourth quarter of FY 97. In this quarter, monitoring of the cooling phase continues.

Electrical Resistance Tomography

Electrical resistance tomography (ERT) is a geophysical imaging technique which can be used to map subsurface resistivity. Rock mass heating creates temperature and liquid saturation changes which result in electrical resistivity changes that are readily measured. The ERT

measurements consist of a series of voltage and current measurements from buried electrodes using an automated data collection system. The data are then processed to produce electrical resistivity tomographs using state of the art data inversion algorithms. We use these measurements to calculate tomographs that show the spatial distribution of the subsurface resistivities.

Here we describe briefly some of the important features of the two dimensional (2D) algorithm. For additional details, the reader is referred to Morelli and LaBrecque (1996). The algorithm solves both the forward and inverse problems. The forward problem is solved using a finite element technique in 2D. The inverse problem implements a regularized solution which minimizes an objective function. The objective of the inverse routine is to minimize the misfit between the forward modeling data and the field data, and a stabilizing functional of the parameters. The stabilizing functional is the solution's roughness. This means that the inverse procedure tries to find the smoothest resistivity model which fits the field data to a prescribed tolerance. Resistivity values assigned in this way to the finite element mesh constitute the ERT image. Although the mesh is of a large region around the electrode arrays, only the region inside the ERT electrode array is shown in the results because the region outside the array is poorly constrained by the data.

To calculate the changes in the rock's electrical resistivity we compared a data set obtained after heating started, and a corresponding data set obtained prior to heating. One may consider subtracting, pixel by pixel images from two different conditions. However, this approach could not be used because the resistivity structure was three-dimensional, i.e., several boreholes containing metallic instruments, were located near the plane of interest (see Figure 1). These metallic instruments caused large conductive anomalies and made the resistivity structure three dimensional (3D). The finite element forward solver cannot generate a model that will fit the data so the code chooses a solution with a poor fit. Our experience is that these effects can be reduced by inverting the quantity:

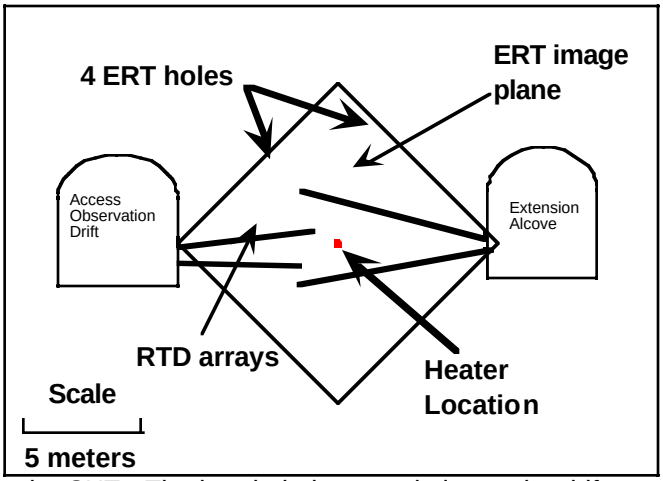

Figure 1. ERT at the SHT. The borehole layout relative to the drifts and the RTD boreholes is shown.

$$\frac{R_a}{R_b} \times R_h \qquad (1)$$

where R_a is the measured transfer resistance after heating started, R_b is the transfer resistance before heating and R_h is the calculated transfer resistance for a model of uniform resistivity. This approach tends to reduce the effects of anomalies which do not match the 2D assumptions of the resistivity model because the 3D effects cancel in the ratio since they are contained in both terms R_a and R_b.

The tomographs presented in this report were calculated in a somewhat different manner than tomographs submitted previously. The data used for the tomographs in this report was the average of three consecutive data sets. That is, each reading used for the tomographs was the average value of the reading measured in three consecutive field surveys. We did this in order to improve the signal to noise ratio of the measurements made at low voltages.

Changes in Resistivity

The changes in electrical resistivity obtained in this quarter are shown in the left hand column of images in Figure 2. The image collected on 5/22/97 show the resistivity changes observed near the end of the heating phase (5/28/97). Note that a "inverted L" shaped resistivity decrease region (indicated by resistivity ratios less than 1.0) is located near the heater location. Twelve days into the cooling phase, the upper tip of this region has disappeared; a region of resistivity increase (ratios greater than 1.0) begins to develop near the heater . After 29 days of cooling, the zone of resistivity increases near the heater grows in size and continues growing in subsequent images. Note that this resistive anomaly is not centered on the heater, probably because of heterogeneous effects in the rockmass (notably fractures). Also, the regions of decreased resistivity observed below the heater became smaller in size as cooling progressed.

Interpretation of moisture content based on resistivity changes is complicated by several factors. First, both moisture content and temperature affect the resistivity mapped by ERT. Fortunately, we have a measure of temperature so that it is possible in principle to separate the two effects and we will attempt this in the next section. Second, our ERT inversion assumes the resistivity structure is strictly two dimensional such that the resistivity varies in the image plane but is constant perpendicular to the image plane (constant parallel to the heater axis). Therefore, the 2D assumption in our ERT model would probably degrade the correlation between ERT image anomalies and fracture location (even if we had fracture maps for the rockmass volume).

During heating there were competing effects at work, i.e., temperature increases caused resistivity decreases while drying caused resistivity increases. Just before the end of the heating phase, the dominant effect was the resistivity decrease due to temperature. This changed by 6/26/97 when the local region about 1 meter to the left of the heater is more resistive than initial conditions. As the temperature decreased to near 50 C, the water resistivity returns toward

higher values; in addition, drying during the heating phase reduced bulk moisture content near the heater. The net effect is that during cooling the resistivity increased.

Inferences of Moisture Changes from ERT

The resistivity changes in Figure 2 are influenced by changes in both moisture content and temperature: an increase in temperature or moisture causes a resistivity decrease. However, near the heater there may be regions where the increasing temperature which reduces the resistivity, acts opposite to the rock drying which increases the resistivity. Our goal in this section is to use the images of resistivity change near the heater, along with the measured temperature field (shown in the second column of Figure 2) and what is known of initial conditions in the rockmass to estimate moisture change during heating.

In order to estimate moisture content changes, we need to account for both effects of temperature, measured at many points by temperature sensors, and resistivity changes, measured by ERT. This is possible by either using laboratory data establishing the relations between moisture, temperature and resistivity or by using a suitable model of electrical conduction in porous media. Roberts and Lin (1997) have published data on the resistivity of Topopah Spring tuff as a function of moisture content. There is, however, limited data on temperature dependence (up to 95 C) and the samples were not from the SHT alcove so that direct use of this data is not simple.

On the other hand, Waxman and Thomas (1954 a, 1954 b) describe a model for electrical conduction in partially saturated shales (intended for oil field data) which accounts for conduction through the bulk pore water as well as conduction through the electrical double layer near the pore surface. This model can predict temperature dependence of the resistivity but several of the model parameters are empirically determined and not available for tuff. Roberts and Lin suggest that the Waxman Smits model provides reasonably good estimates of resistivity for saturations greater than 20%. For saturations less than 20%, their data shows that the Waxman Smits model substantially under predicts the resistivity. We will use this model to account for the temperature effects on the resistivity changes and to estimate changes in rock saturation. Details pertaining to the Waxman Smits model can be found in reports submitted for the 2nd and 3rd quarter of FY 97.

We used the available temperature data to construct temperature maps along the ERT image plane. It is necessary to have a reliable temperature measurement for each area (each tomograph pixel) were we wish to calculate the saturation change. At the SHT, there are many temperatures sensors located along roughly horizontal boreholes. However, the temperature coverage in the vertical direction is sparse extending only +/- 1.7 m away from the heater. In order to construct temperature maps we were forced to extrapolate vertically out to +/- 6.3 m away from the heater. It was necessary to assume that the vertical temperature gradient equaled the horizontal gradient in order to obtain physically reasonable temperature values for regions beyond 1.7 m vertically. Thus, the accuracy of the temperature maps is expected to be good along the horizontal direction but may be in error along the vertical direction for regions farther than 1.7 meters from the heater.

The ERT images provide a measure of change in resistivity from baseline (through the resistivity ratio). We have chosen two simplifications of the Waxman-Smits model to provide a range of possible saturations estimates. This approach should provide bounds to the domain of possible saturations that may be present. Available data suggests that the welded tuff at the SHT should show behavior closer to model 2 than to model 1. However, if the cation exchange capacity, porosity or water resistivity varied significantly from the quantities assumed, it is possible that model 1 results may be closer to reality. The results of these saturation estimates are discussed next.

Saturation estimates reported in the previous report cover data collected from before heating to 6/26/97. The third and fourth column of images in Figure 2 shows estimates of saturation based on the resistivity ratios obtained during this reporting period and the second column in Figure 2 shoes the interpolated/extrapolated maps of temperature used for the model calculations. For the calculation we assume that initial saturation (S_b) of the rock unit was uniform and 0.92; this is the average saturation from core samples collected at the experimental site and reported by Wagner (1996).

Both models indicate dehydration around the heater. Model 2 generally predicts substantially drier saturations near the heater than model 1; model 2 saturations near the heater are closer to a priori expectations than those from model 1. The dry zone is not centered on the heater and certainly not symmetric about the heater. The pattern is suggestive to us of distribution of moisture which is strongly controlled by fractures. During the cooling phase, the dry zone around the heater appears to remain relatively stable.

Dehydration appears highest in regions above the heater whereas moisture accumulation appears prevalent in regions below. (In some patches the saturation is calculated to be greater than 1.0, clearly a nonphysical condition, as the rock can be no more than fully saturated. It is possible that those regions began dryer than the 0.92 saturation level assumed to be the initial conditions for the calculation.) The zones near full saturation are mostly located below the heater at the seven o'clock and eight o'clock positions.

The lowest imaged moisture content is on 5/23/97, the last ERT data before the heater was turned off. As the temperature field collapses during the first 29 days of cool down, that extremely dry region, about 0.2 saturation for model 2, appears to be slowly rewetting. The rest of the dehydrated zone, appears stable except for minor changes which imply that water is still moving in the rockmass.

Regions showing saturations near 1.0 appear primarily below the heater. On 5/23/97 these regions cover a significant portion of the area below the heater. By 6/26/97, these regions appear somewhat smaller suggesting that some of the water is leaving this area. After the 6/26/97 images the wet regions below and above the heater appear to be stable. The data from 9/25/97 indicates a change from the trend above the heater, i.e., above the heater, at the two o'clock position, a couple of small regions show increased moisture content. It is interesting that

wet regions at the two and eight o'clock positions on the 9/25 data are aligned with a region near the heater that did not dry as much during the course of the heating phase. This pattern suggests the possibility that a fracture or fracture zone is bringing moisture to dry regions near the heater.

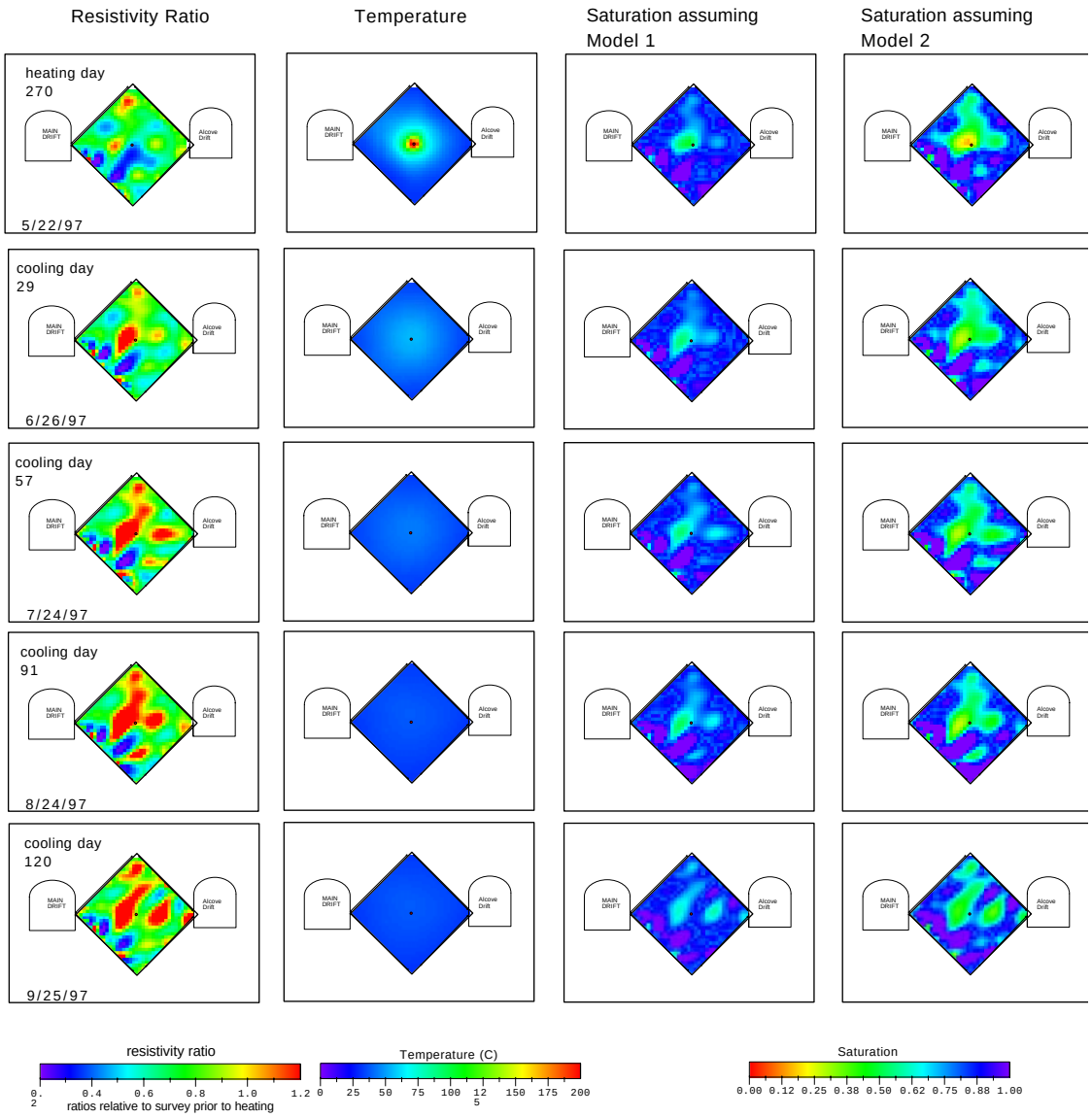

Technical Information Department • **Lawrence Livermore National Laboratory**
University of California • Livermore, California 94551